

constant. The observed temperature hysteresis of the VI-VII transition becomes insignificant as pressure increases. Figure 5 shows the pressure dependence of the square root of the

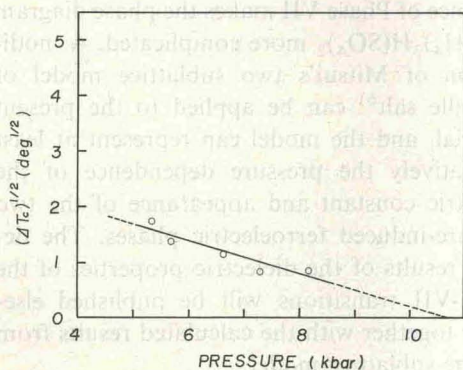


Fig. 5. Pressure dependence of the square root of the thermal hysteresis of the VI-VII transition $(\Delta T_c)^{1/2}$ in $(\text{NH}_4)_3\text{H}(\text{SO}_4)_2$.

thermal hysteresis $(\Delta T_c)^{1/2}$ of the VI-VII transition. It is noted that the thermal hysteresis of the VI-VII transition tends to disappear at around 11 kbar. Then, the transition will be a continuous one at higher pressures. Since our arrangement did not realize pressures above 10 kbar, we did not directly observe the critical point at which the first order character of the VI-VII transition disappears.

§4. Discussion and Conclusion

The pressure-temperature phase diagram of $(\text{NH}_4)_3\text{H}(\text{SO}_4)_2$ obtained in the present work is shown in Fig. 6. The present work did not observe the pressure dependence of the lower temperature phase transitions of the III-IV and IV-V. Preliminary X-ray measurements of the thermal expansion showed that both the III-IV and the IV-V transitions should

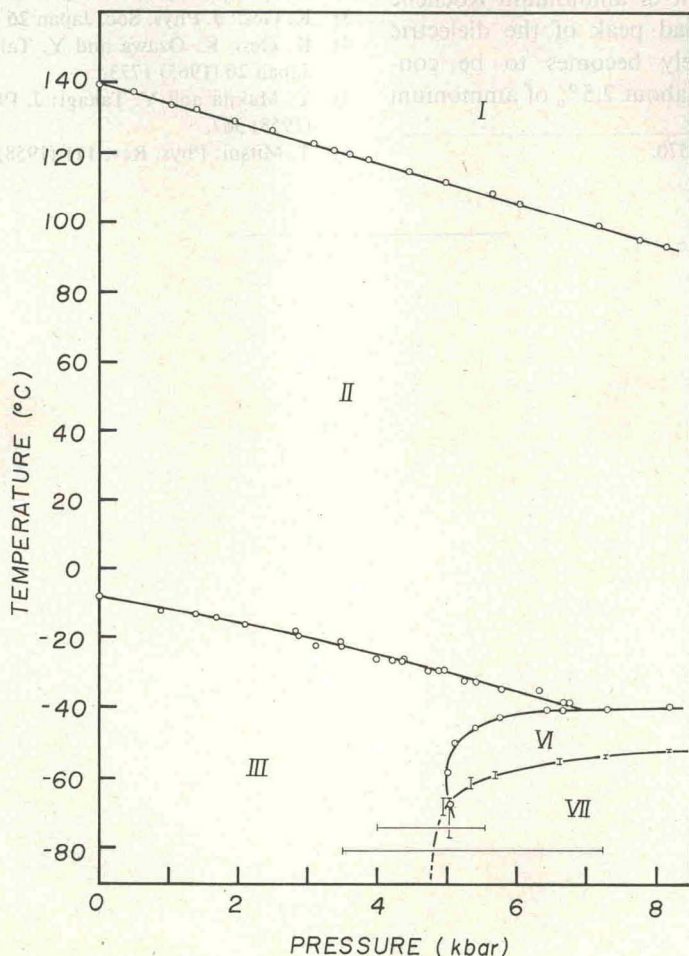


Fig. 6. Pressure-temperature phase diagram of $(\text{NH}_4)_3\text{H}(\text{SO}_4)_2$.

increase with increasing pressure.* However, the pressure-induced phases VI and VII are not identical with any of the low temperature phases IV and V which are not ferroelectric. Thus, the phase diagram below -100°C is a remaining problem. Suzuki *et al.** observed a discontinuous volume change for the I-II transition $\Delta v/v = -7.6 \times 10^{-3}$ at 1 atm. By using the Clausius-Clapeyron relation of $Q_L = (T_c \cdot (\Delta v/v)) / (dT_c/dp)$ together with the observed $dT_c/dp = -5.76 \text{ deg kbar}^{-1}$, $T_c = 413 \text{ K}$, one may get the latent heat Q_L of the I-II transition to be $1.75 \times 10^3 \text{ cal mol}^{-1}$.

The existence of the pressure-induced ferroelectric phases of VI and VII characterizes the phase diagram of $(\text{NH}_4)_3\text{H}(\text{SO}_4)_2$. There is a similarity between the pressure-temperature phase diagram of the present material and the phase diagram of Rochelle salt-ammonium Rochelle salt system.⁵⁾ In the latter system as the content of ammonium Rochelle salt decreases a broad peak of the dielectric constant progressively becomes to be conspicuous, and below about 2.5% of ammonium

Rochelle salt contents the peak of the dielectric constant splits into two peaks. Then, a ferroelectric phase appears between them. The situation is quite similar to that observed in the present compound²⁾ although the appearance of Phase VII makes the phase diagram of $(\text{NH}_4)_3\text{H}(\text{SO}_4)_2$ more complicated. A modification of Mitsui's two sublattice model of Rochelle salt⁶⁾ can be applied to the present material, and the model can represent at least qualitatively the pressure dependence of the dielectric constant and appearance of the two pressure-induced ferroelectric phases. The detailed results of the dielectric properties of the III-VI-VII transitions will be published elsewhere together with the calculated results from two the sublattice model.

References

- 1) K. Gesi: Phys. Status solidi (a) **33** (1976) 479.
- 2) K. Gesi: J. Phys. Soc. Japan **41** (1976) 1437.
- 3) K. Gesi: J. Phys. Soc. Japan **26** (1969) 107.
- 4) K. Gesi, K. Ozawa and Y. Takagi: J. Phys. Soc. Japan **20** (1965) 1773.
- 5) Y. Makita and Y. Takagi: J. Phys. Soc. Japan **13** (1958) 367.
- 6) T. Mitsui: Phys. Rev. **111** (1958) 1259.

* See footnote in p. 570.

